ADP-15-29/T931, DESY 15-156, Edinburgh 2015/21, LTH 1056

# Disconnected contributions to the spin of the nucleon

A. J. Chambers,[1] R. Horsley,[2] Y. Nakamura,[3] H. Perlt,[4] D. Pleiter,[5,6] P. E. L. Rakow,[7] G. Schierholz,[8] A. Schiller,[4] H. Stüben,[9] R. D. Young,[1] and J. M. Zanotti[1]

[1] *CSSM, Department of Physics, University of Adelaide, Adelaide SA 5005, Australia**
[2] *School of Physics and Astronomy, University of Edinburgh, Edinburgh EH9 3JZ, UK*
[3] *RIKEN Advanced Institute for Computational Science, Kobe, Hyogo 650-0047, Japan*
[4] *Institut für Theoretische Physik, Universität Leipzig, 04103 Leipzig, Germany*
[5] *JSC, Jülich Research Centre, 52425 Jülich, Germany*
[6] *Institut für Theoretische Physik, Universität Regensburg, 93040 Regensburg, Germany*
[7] *Theoretical Physics Division, Department of Mathematical Sciences, University of Liverpool, Liverpool L69 3BX, UK*
[8] *Deutsches Elektronen-Synchrotron DESY, 22603 Hamburg, Germany*
[9] *Regionales Rechenzentrum, Universität Hamburg, 20146 Hamburg, Germany*

arXiv:1508.06856v1 [hep-lat] 27 Aug 2015

The spin decomposition of the proton is a long-standing topic of much interest in hadronic physics. Lattice QCD has had much success in calculating the connected contributions to the quark spin. However, complete calculations, which necessarily involve gluonic and strange-quark contributions, still present some challenges. These "disconnected" contributions typically involve small signals hidden against large statistical backgrounds and rely on computationally intensive stochastic techniques. In this work we demonstrate how a Feynman-Hellmann approach may be used to calculate such quantities, by measuring shifts in the proton energy arising from artificial modifications to the QCD action. We find a statistically significant non-zero result for the disconnected quark spin contribution to the proton of about $-5\%$ at a pion mass of 470 MeV.

## I. INTRODUCTION

The simple quark model picture suggests that the total nucleon spin is comprised entirely in terms of its constituent quark spins. In contrast, experimental measurements reveal that the quark spin only generates about one third of the total nucleon spin [1]. This observation is a clear representation of the nontrivial dynamics associated with nonperturbative QCD. Resolving the full composition of the nucleon spin in terms of the QCD degrees of freedom remains an active experimental and theoretical pursuit. For an overview of the status and progress, we refer the reader to Refs. [2–7].

As a systematically improvable method for studying nonperturbative properties of QCD, lattice simulations offer the potential to provide quantitative predictions for the decomposition of the nucleon spin. For recent numerical investigations of the nucleon spin, and related matrix elements, see Refs. [8–16].

In the conventional approach, spin matrix elements are extracted from 3-point correlation functions. Operator insertions that are directly connected to the quark field operators of the nucleon interpolators can be reliably computed using established techniques. The operator insertions that involve self-contracted fermion lines, which are essential to isolate the strangeness spin content, for instance, require the stochastic estimation of the trace of an all-to-all propagator. Owing to the increased computational demand of this stochastic estimator and a relatively weak numerical signal, such disconnected contributions have often been neglected in lattice simulations. Nevertheless, there has been substantial progress made in recent years [17–21]. For a related calculation involving the vector current matrix elements we also refer to Ref. [22].

In recent work, we have proposed an alternative to the conventional 3-point function technique for the study of hadron matrix elements in lattice QCD. By adapting the Feynman-Hellmann (FH) theorem to the lattice framework, we are able to isolate matrix elements in terms of an energy shift in the presence of an appropriate weak external field [23, 24]. This is similar to the technique proposed by Detmold in Ref. [25]. In Ref. [23] we used the Feynman-Hellmann relation to extract the gluonic contribution to the nucleon mass. The application of Feynman-Hellmann was further developed in Ref. [24] for the study of the connected spin contributions in various hadrons. We have also recently shown how it is possible to compute flavour-singlet renormalisation constants nonperturbatively by an appropriate application of the FH theorem [26].

In the present work, we apply the FH technique to resolve disconnected spin matrix elements. Whereas the connected spin contributions could be computed on conventional gauge fields, the disconnected contributions requires the generation of new special-purpose gauge configurations. The influence of the weak external spin field is therefore accumulated through the importance sampling of the hybrid Monte Carlo simulation. While such new configurations come at significant computational cost, the computing time is comparable to that required for reliable with sampling using the conventional stochastic techniques.

The manuscript proceeds as follows: Section II reviews the implementation of the FH theorem for the extraction

* alexander.chambers@adelaide.edu.au

of spin matrix elements and summarises the lattice simulation parameters; Section III describes the strategy for the isolation of the relevant matrix elements from the two-point correlation functions; with results reported in Section IV; followed by concluding remarks in Section V.

## II. FEYNMAN-HELLMANN METHODS AND SIMULATION DETAILS

Here we discuss the Feynman-Hellmann approach in the context of calculations of disconnected contributions to matrix elements, in particular the quark axial charges. For details of previous calculations of the connected contributions, and the Feynman-Hellmann technique in general, see [24].

The quark axial charges are defined by forward matrix elements of the axial operator,

$$\langle \vec{p}, \vec{s} \,|\, \bar{q}(0)\gamma_\mu\gamma_5 q(0) \,|\, \vec{p}, \vec{s} \rangle = 2is_\mu \Delta q \,. \tag{1}$$

We access disconnected contributions to these quantities by implementing a modification to the fermion part of the QCD Lagrangian during gauge-field generation. Extra terms are included involving the axial operator weighted by some freely-varying real parameter $\lambda$, applied equally to all three quark flavours,

$$\mathcal{L} \to \mathcal{L} + \lambda \sum_{q=u,d,s} \bar{q}\gamma_3\gamma_5 q \,. \tag{2}$$

This operator satisfies $\gamma_5$-hermiticity, and so the determinant of the fermion matrix is still real. Hence we avoid introducing any sign problems. We choose projection matrices to isolate spin-up and down components of the nucleon correlation function,

$$\Gamma_\pm = \frac{1}{2}(\mathbb{I} + \gamma_4)\frac{1}{2}(\mathbb{I} \pm i\gamma_5\gamma_3) \,, \tag{3}$$

and by application of the Feynman-Hellmann relation, find that the correlator picks up a complex phase which mimics an imaginary energy component,

$$E \to E(\lambda) + i\phi(\lambda) \,. \tag{4}$$

At first order in the parameter $\lambda$, there is no shift in the real part of the energy, and the shift in the phase is exactly equal to the disconnected contribution to the total quark axial charge,

$$\left.\frac{\partial E}{\partial \lambda}\right|_{\lambda=0} = 0 \qquad \left.\frac{\partial \phi}{\partial \lambda}\right|_{\lambda=0} = \pm\Delta\Sigma_{\text{disc.}} \,, \tag{5}$$

where the total contribution is the sum of the individual flavour contributions,

$$\Delta\Sigma_{\text{disc.}} = \Delta u_{\text{disc.}} + \Delta d_{\text{disc.}} + \Delta s \,. \tag{6}$$

Note that we access the total contribution because the operator in Eq. (2) includes terms for all 3 quark flavours. Also note that the strange contribution is purely disconnected. The different signs in Eq. (5) result from the different choices of $\Gamma_\pm$, and we note that changing the spin projection is equivalent to flipping the sign of $\lambda$.

Our strategy for this calculation, motivated by Eq. (5), is to generate new gauge ensembles for multiple values of $\lambda$, measure the phase shift in Eq. (4) and determine $\Delta\Sigma_{\text{disc.}}$ from the linear behaviour.

In our previous work, we were able to access the connected part by implementing the change in Eq. (2) to the Dirac matrix before inversion to compute the quark propagator entering hadron correlation functions (see [24]). Here the modification is made to the fermion matrix in the HMC algorithm, and so information about the purely disconnected contributions is accessed.

| $(\kappa_l, \kappa_s)$ | $\lambda$ | $N_{\text{conf.}}$ | $N_{\text{sources}}$ | $\phi$ |
|---|---|---|---|---|
| (0.120900, 0.120900) | -0.0125 | 500 | 1 | 0.0014(10) |
| | -0.00625 | 500 | 1 | 0.00002(83) |
| | 0.03 | 500 | 1 | -0.00237(77) |
| (0.121095, 0.120512) | -0.025 | 600 | 1 | -0.0008(13) |
| | 0.05 | 800 | 5 | 0.00027(61) |

TABLE I. Table of ensembles generated for this work. Two pion masses with three and two values of $\lambda$ respectively have been used. The number of configurations and sources used, as well as the phase shift measured (discussed in Sec. III and Sec. IV) are also listed.

### A. Simulation details

We use gauge field configurations with $2+1$ flavours of non-perturbatively $O(a)$-improved Wilson fermions and a lattice volume of $L^3 \times T = 32^3 \times 64$. The lattice spacing $a = 0.074(2)$ fm is set using a number of singlet quantities [27–30]. The clover action used comprises the tree-level Symanzik improved gluon action together with a stout smeared fermion action, modified for the implementation of the Feynman-Hellmann method [24].

For the results discussed here, we use ensembles with two sets of hopping parameters, $(\kappa_l, \kappa_s) =$ (0.120900,120900) and (0.121095,0.120512), corresponding to pion masses of approximately 470 and 310 MeV. These have been generated with the modified quark action described in Eq. (2). The details of these ensembles, including the values of $\lambda$ realised, are given in Table I.

## III. ANALYSIS TECHNIQUES

A standard zero-momentum projected nucleon correlation function is given by

$$G_\pm(t) = \int \mathrm{d}^3\vec{x}\, \Gamma_\pm \langle\, \Omega \,|\, N(x)\bar{N}(0) \,|\, \Omega \,\rangle \xrightarrow{\text{large } t} Ae^{-Et} \,,$$

where $N$ and $\bar{N}$ are interpolating operators coupling to the nucleon ground state, and the projection matrices $\Gamma_\pm$ (defined in Eq. (3)) project spin-up and down components respectively. For our simulations, we use identical source and sink smearing and operators. Hence, the amplitude $A$ is purely real.

With the modification to the Lagrangian in Eq. (2), an imaginary component is introduced to the exponential factor, in addition to a complex shift in the amplitude. This shift in the amplitude is not the focus of this work, but is related to the $\lambda$ dependence of the wavefunction overlap factors. To first order in $\lambda$, the amplitude and energy take the form

$$A \to A + \lambda(\Delta A + i\Delta B)\,, \tag{7}$$
$$E \to E + i\lambda\Delta\Sigma\,, \tag{8}$$

and the correlation function at large times is given by

$$G_\pm(\lambda,t) \xrightarrow{\text{large } t} [A \pm \lambda(\Delta A + i\Delta B)]\, e^{-[E\pm i\lambda\Delta\Sigma]t}\,. \tag{9}$$

(Recall that changing the spin projection corresponds to flipping the sign of $\lambda$, as discussed in Sec. II). The quantity of interest is the shift in the phase, $\Delta\Sigma$. To extract this value, we form the following ratio of real and imaginary parts of spin-up and down projections,

$$\begin{aligned} R(\lambda,t) &= \frac{\mathrm{Im}\left[G_-(\lambda,t) - G_+(\lambda,t)\right]}{\mathrm{Re}\left[G_-(\lambda,t) + G_+(\lambda,t)\right]} \\ &\xrightarrow{\text{large } t} \frac{\sin\left(\lambda\Delta\Sigma t\right) - \lambda\frac{\Delta B}{A}\cos\left(\lambda\Delta\Sigma t\right)}{\cos\left(\lambda\Delta\Sigma t\right) + \lambda\frac{\Delta B}{A}\sin\left(\lambda\Delta\Sigma t\right)}\,. \end{aligned} \tag{10}$$

Note that the form of this ratio does not change if we include second order terms in Eq. (7) and Eq. (8). For the operator included in Eq. (2), we find that the second order shift in the energy is purely real, and it can be shown that only the factor $\frac{\Delta B}{A}$ will change. Hence, corrections to these calculations do not appear until $\mathcal{O}\left(\lambda^3\right)$.

The ratio in Eq. (10) is what we fit in our analysis. To determine ground state saturation of this quantity, we observe that, provided $t \ll \frac{1}{|\lambda\Delta\Sigma|}$, the behaviour of the ratio is approximately linear in $t$.

$$R(\lambda,t) = \lambda\Delta\Sigma t - \lambda\frac{\Delta B}{A} + \mathcal{O}\left(\lambda^3\right) \quad , \quad a \ll t \ll \frac{1}{|\lambda\Delta\Sigma|}\,. \tag{11}$$

Previous determinations of $\Delta\Sigma$ [17–21] suggest that we should expect $|\Delta\Sigma| \approx 0.1$, and hence for the largest value of $\lambda$ realised on our ensembles, $a\lambda = 0.05$, this linear approximation will hold for times $\frac{t}{a} \ll 200$. With this, we are able to introduce an 'effective phase shift',

$$\phi_{\text{eff.}} = \frac{1}{a}\left[\mathcal{R}(\lambda,t+a) - \mathcal{R}(\lambda,t)\right] \tag{12}$$

which in the regime discussed has the behaviour

$$\phi_{\text{eff.}} = \lambda\Delta\Sigma \quad , \quad a \ll t \ll \frac{1}{|\lambda\Delta\Sigma|}\,. \tag{13}$$

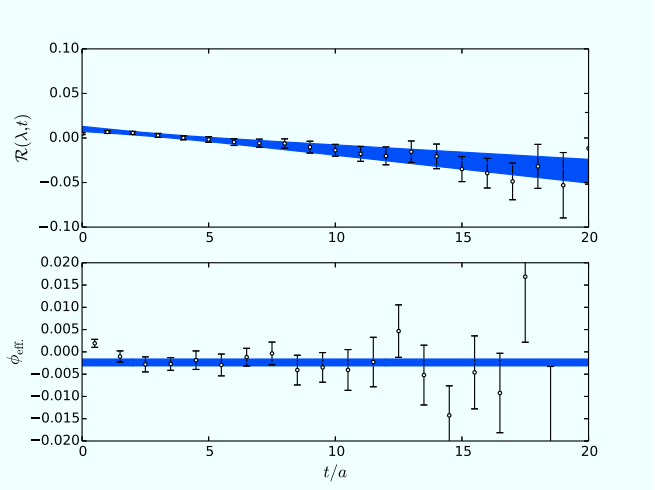


FIG. 1. Plots of the ratio in Eq. (10) and the effective phase shift defined in Eq. (13) for $\lambda = 0.03$, $m_\pi \approx 470$ MeV. The fitting window (shown in darker blue) was between time slices 2 and 12. The errors shown are from a bootstrap analysis of the results, as are the errors on the displayed fits.

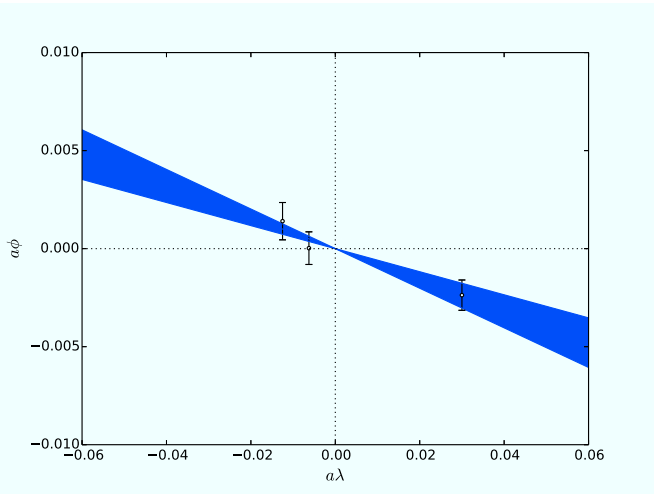


FIG. 2. Phase shift as a function of $\lambda$ for $m_\pi \approx 470$ MeV.

## IV. RESULTS

Fig. 1 shows an example plot of the ratio in Eq. (10) and the corresponding effective phase defined in Eq. (13) for $\lambda = 0.03$. We observe a clear plateau in the effective phase for the illustrated fitting region, and corresponding linear behaviour in the ratio. As an aside, the fit indicates a clearly non-zero value for the $t = 0$ intercept, confirming that there is a small but statistically significant imaginary shift in the wavefunction overlap factors (given in Eq. (7)) for this value of $\lambda$.

Repeating this procedure for each value of $\lambda$ and extracting the phase shifts, we are able to calculate the linear shift with respect to $\lambda$, illustrated in Fig. 2. From Eq. (5) we know that this shift is directly proportional to

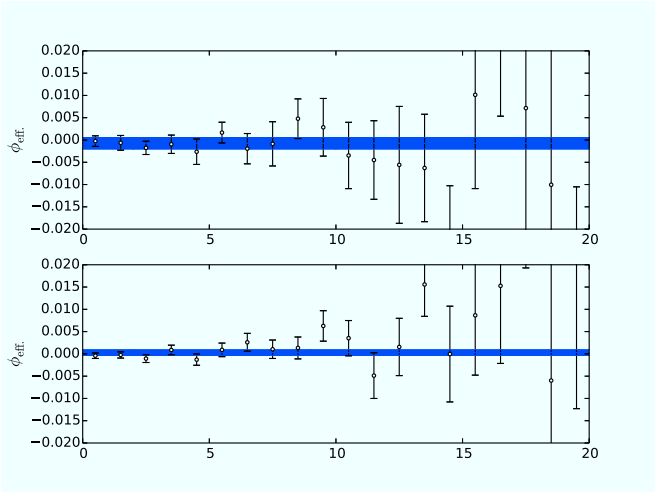


FIG. 3. Effective phase plots for $\lambda = -0.025, 0.05$ respectively at $m_\pi \approx 310$ MeV. The results in the second plot have greater statistics by a factor of 4. Note that the sign of the fitted value is highly dependent on the fit window.

the disconnected contribution to $\Delta\Sigma$. Since there is no phase shift in the zero-field limit, we have used a single-parameter slope fit to extract the linear shift. This analysis is repeated at the lighter pion mass. Table I includes the calculated phase shift for each value of $\lambda$ on the ensembles generated, and results of the described analyses are summarised in Table II. Using the methods outlined in [24], we have also calculated the individual connected contributions to $\Delta\Sigma$ on these ensembles, and hence are able to calculate the total (connected and disconnected) value of $\Delta\Sigma$.

At the lighter mass, we find a result consistent with zero for $\Delta\Sigma_{\text{disc.}}$. This unusual result may be the result of a couple of different factors. The $\lambda$ values chosen may simply be too small, and the phase shift is not able to rise above the background correlator noise. Fig. 3 show effective phase plots for the two values of $\lambda$ realised at this lighter quark mass, and show that there is no clearly identifiable plateau at these statistics.

Alternatively, there may be a sign change in either the light or strange contribution to $\Delta\Sigma$ at some mass between $m_\pi = 310 - 470$ MeV. This is unlikely, however, as previous results at similar masses have shown a significant $\Delta s$ contribution, which would require the light quark contribution to have a strong quark mass dependence.

From [26] we have both non-singlet and singlet renormalisation factors for the axial current at the SU(3) symmetric point,

$$Z_{A,\text{NS}}^{\overline{\text{MS}}(2\text{ GeV}^2)} = 0.8458(8)\,, \tag{14}$$

$$Z_{A,\text{S}}^{\overline{\text{MS}}(2\text{ GeV}^2)} = 0.8662(34)\,. \tag{15}$$

Further calculations at additional quark masses are required to perform a chiral extrapolation of these quantities, however the pion mass dependence of these factors is expected to be mild based on the non-singlet calculation of Ref. [31].

To obtain the renormalised total spin contribution we use the singlet renormalisation factor:

$$\Delta\Sigma^{\overline{\text{MS}}} = Z_{A,\text{S}}^{\overline{\text{MS}}}\Delta\Sigma^{\text{latt.}}. \tag{16}$$

For the purely disconnected quantity, we include the mixing of the connected and disconnected contributions under renormalisation:

$$\Delta\Sigma_{\text{disc.}}^{\overline{\text{MS}}} = Z_{A,\text{S}}^{\overline{\text{MS}}}\Delta\Sigma_{\text{disc.}}^{\text{latt.}} + \left(Z_{A,\text{S}}^{\overline{\text{MS}}} - Z_{A,\text{NS}}^{\overline{\text{MS}}}\right)\Delta\Sigma_{\text{conn.}}^{\text{latt.}}\,. \tag{17}$$

Using the renormalisation factors from the SU(3) symmetric point, we quote our $\overline{\text{MS}}$ results in the final two columns of Table II.

Finally, since at the SU(3) symmetric point all quarks contribute exactly the same amount to $\Delta\Sigma_{\text{disc.}}^{\overline{\text{MS}}}$, then at this point we can determine $\Delta s$

$$\Delta s^{\overline{\text{MS}}}(m_\pi = 465\text{MeV}) = \frac{1}{3}\Delta\Sigma_{\text{disc.}}^{\overline{\text{MS}}} = -0.018(6)\,. \tag{18}$$

## V. CONCLUDING REMARKS

Culminating in the results of Table II, we have shown how the Feynman-Hellmann theorem may be applied to perform full calculations of hadronic matrix elements.

Extensions of these particular calculations include higher-statistics simulations, particularly at the lighter pion mass, and the generation of ensembles at additional pion masses to identify the quark mass dependence of $\Delta\Sigma$. Further analysis of the existing data should allow for the extraction of disconnected quark spin contributions for the other octet baryons and the vector mesons.

The FH technique demonstrated here can be easily adapted to a variety of other disconnected quantities, such as the gluonic contribution to angular momentum, which would otherwise be rather challenging using conventional approaches.

## ACKNOWLEDGEMENTS

The numerical configuration generation was performed using the BQCD lattice QCD program, [32], on the IBM BlueGeneQ using DIRAC 2 resources (EPCC, Edinburgh, UK), the BlueGene P and Q at NIC (Jülich, Germany) and the Cray XC30 at HLRN (Berlin–Hannover, Germany). Some of the simulations were undertaken using resources awarded at the NCI National Facility in Canberra, Australia, and the iVEC facilities at the Pawsey Supercomputing Centre. These resources are provided through the National Computational Merit Allocation Scheme and the University of Adelaide Partner Share supported by the Australian Government. The BlueGene codes were optimised using Bagel [33]. The

| $(\kappa_l, \kappa_s)$ | $\Delta u^{\text{latt.}}$ | $\Delta d^{\text{latt.}}$ | $\Delta\Sigma^{\text{latt.}}_{\text{disc.}}$ | $\Delta\Sigma^{\text{latt.}}$ | $\Delta\Sigma^{\overline{\text{MS}}(2\text{ GeV}^2)}_{\text{disc.}}$ | $\Delta\Sigma^{\overline{\text{MS}}(2\text{ GeV}^2)}$ |
|---|---|---|---|---|---|---|
| (0.120900, 0.120900) | 1.001(7) | −0.310(5) | −0.079(21) | 0.612(24) | −0.055(18) | 0.530(21) |
| (0.121095, 0.120512) | 1.004(10) | −0.319(6) | 0.014(16) | 0.699(25) | 0.026(14) | 0.605(21) |

TABLE II. Table of results at each pion mass for the individual quark axial charges and the disconnected and full (connected plus disconnected) contribution to the total quark spin. The quantities reported with the "latt." superscript are unrenormalised. The final two columns report our renormalised results based upon Eqs. (14) through (17).

Chroma software library [34], was used in the data analysis. This investigation has been supported by the Australian Research Council under grants FT120100821, FT100100005 and DP140103067 (RDY and JMZ). HP was supported by DFG grant SCHI 422/10-1.

[1] COMPASS Collaboration, V. Y. Alexakhin *et al.*, Phys. Lett. **B647**, 8 (2007), hep-ex/0609038.
[2] M. Anselmino, A. Efremov, and E. Leader, Phys. Rept. **261**, 1 (1995), hep-ph/9501369.
[3] B. W. Filippone and X.-D. Ji, Adv. Nucl. Phys. **26**, 1 (2001), hep-ph/0101224.
[4] S. D. Bass, Rev. Mod. Phys. **77**, 1257 (2005), hep-ph/0411005.
[5] F. Myhrer and A. W. Thomas, Phys. Lett. **B663**, 302 (2008), 0709.4067.
[6] A. W. Thomas, Phys. Rev. Lett. **101**, 102003 (2008), 0803.2775.
[7] C. A. Aidala, S. D. Bass, D. Hasch, and G. K. Mallot, Rev. Mod. Phys. **85**, 655 (2013), 1209.2803.
[8] LHPC Collaboration, J. D. Bratt *et al.*, Phys. Rev. **D82**, 094502 (2010), 1001.3620.
[9] S. N. Syritsyn *et al.*, PoS **LATTICE2011**, 178 (2011), 1111.0718.
[10] S. Dinter *et al.*, Phys. Lett. **B704**, 89 (2011), 1108.1076.
[11] B. J. Owen *et al.*, Phys. Lett. **B723**, 217 (2013), 1212.4668.
[12] S. Capitani *et al.*, Phys. Rev. **D86**, 074502 (2012), 1205.0180.
[13] A. Sternbeck *et al.*, PoS **LATTICE2011**, 177 (2011), 1203.6579.
[14] C. Alexandrou *et al.*, Phys. Rev. D **88**, 014509 (2013), 1303.5979.
[15] T. Bhattacharya *et al.*, (2013), 1306.5435.
[16] G. S. Bali *et al.*, (2013), 1311.7041.
[17] R. Babich *et al.*, Phys. Rev. **D85**, 054510 (2012), 1012.0562.
[18] QCDSF Collaboration, G. S. Bali *et al.*, Phys. Rev. Lett. **108**, 222001 (2012), 1112.3354.
[19] M. Engelhardt, Phys. Rev. **D86**, 114510 (2012), 1210.0025.
[20] A. Abdel-Rehim *et al.*, Phys. Rev. **D89**, 034501 (2014), 1310.6339.
[21] M. Deka *et al.*, (2013), 1312.4816.
[22] J. Green *et al.*, (2015), 1505.01803.
[23] QCDSF/UKQCD Collaborations, R. Horsley *et al.*, Phys. Lett. **B714**, 312 (2012), 1205.6410.
[24] A. Chambers *et al.*, Phys. Rev. **D90**, 014510 (2014), 1405.3019.
[25] W. Detmold, Phys. Rev. **D71**, 054506 (2005), hep-lat/0410011.
[26] A. Chambers *et al.*, Phys. Lett. **B740**, 30 (2015), 1410.3078.
[27] R. Horsley *et al.*, PoS **LATTICE2013**, 249 (2013), 1311.5010.
[28] V. G. Bornyakov *et al.*, (2015), 1508.05916.
[29] W. Bietenholz *et al.*, Phys. Lett. **B690**, 436 (2010), 1003.1114.
[30] W. Bietenholz *et al.*, Phys. Rev. **D84**, 054509 (2011), 1102.5300.
[31] M. Constantinou *et al.*, Phys. Rev. **D91**, 014502 (2015), 1408.6047.
[32] Y. Nakamura and H. Stüben, PoS **LATTICE2010**, 040 (2010), 1011.0199.
[33] P. A. Boyle, Comput. Phys. Commun. **180**, 2739 (2009).
[34] SciDAC Collaboration, LHPC Collaboration, UKQCD Collaboration, R. G. Edwards and B. Joo, Nucl. Phys. Proc. Suppl. **140**, 832 (2005), hep-lat/0409003.